The 7th International Supercritical CO_2 Power Cycles Symposium
February 21 –24, 2022, San Antonio, Texas
Paper #13

A Design of 2MW Rated s-CO2 Compressor Test Rig

Zhang Jingxuan
Huang Weiguang
Shanghai Advanced Research Institute (SARI), CAS
Center of Advanced Energy System and Equipment R&D

Francis Di Bella
Kevin Fairman
Alex Gofer, David Karon
Concepts NREC, LLC

ABSTRACT

In recent years, supercritical carbon dioxide (sCO2) power cycle has attracted much more attention for its prominent advantages, such as high efficiency, high-power density and wide range of applications. The performance of the sCO2 compressor plays a very important role in the operation of the whole cycle, especially during the part load operation. Because of the non-ideal gas properties of the sCO2 fluid above and near the critical point, the use of the traditional design code for an sCO2 compressor must be verified with the actual testing of the design and possible modification of the design code. However, there are few industrial application level sCO2 compressor rigs for the experimental research.

In this paper, a 2MW rated sCO2 compressor rig is designed with some test articles considered — test articles include: (1) the compressor impeller, (2) the diffuser, and (3) the volute. This paper will review the final design of the compressor including the AERO and structural design of the sCO2 impeller, as well as a review of the bearings, shaft seal and plans for the instrumentation as required to quantify the performance of the compressor.

SARI (Shanghai Advanced Research Institute) is a multi-disciplinary scientific research institute based in Shanghai, China. SARI is developing a world class sCO2 turbomachinery testing facility. Concepts NREC LLC, known for its turbomachinery software and turbomachinery engineering services, is collaborating with SARI in the development of the compressor rig for SARI's laboratory testing.

1. BACKGROUND

Since 2010, SARI has been working on the key technologies of closed-cycle gas turbine, which has the potential to serve as power conversion system for a wide range of energy sources, especially for the clean energy such as concentrated solar power (CSP) and Gen IV nuclear. Both Helium Turbine and sCO2 cycle researches are carried out with the different aims, helium turbine is for high temperature energy sources such as Very High Temperature Reactor (VHTR) and Molten Salt Reactor (MSR) and sCO2 cycle is for middle or low temperature energy sources such as CSP and waste heat. With the project of "Thorium-based Molten-Salt Reactor (TMSR)" [1] funding, a helium closed Brayton cycle test loop has been developed, and a 10MWth helium turbine prototype has been designed [2]. Currently, SARI is designing and building an sCO2 test loop to investigate the performance of the key components of sCO2 cycle such as compressor, heat exchanger and turbine. The heat sink, drive motor, lubrication oil station and part of measurement system are ones which are also used in the Helium Turbine test loop. In this paper, the 2MW rated compressor test loop is presented and the contents are organized as follows. The design of the test loop and thermodynamic process are first given. The compressor rig including aerodynamic design and structure design is the described. The summaries and discussions are given at the end.

THE DESCRIPTION OF COMPRESSOR TEST LOOP

The purpose of the sCO2 compressor test loop is to characterize the performance of both compressor and high compactness heat exchanger. Therefore, an electric heater is chosen to provide high temperature. Some adjust valves are used to achieve the designed mass flow rate of the heat exchanger. An in-house MATLAB code is applied to calculate the thermodynamic parameters of the test loop, and the maximum work consumption of the compressor is fixed at 2MW due to the limitation of existed drive motor. Fig 1 gives the whole flow chart of the loop, and design point specification for the compressor is shown in Table I.

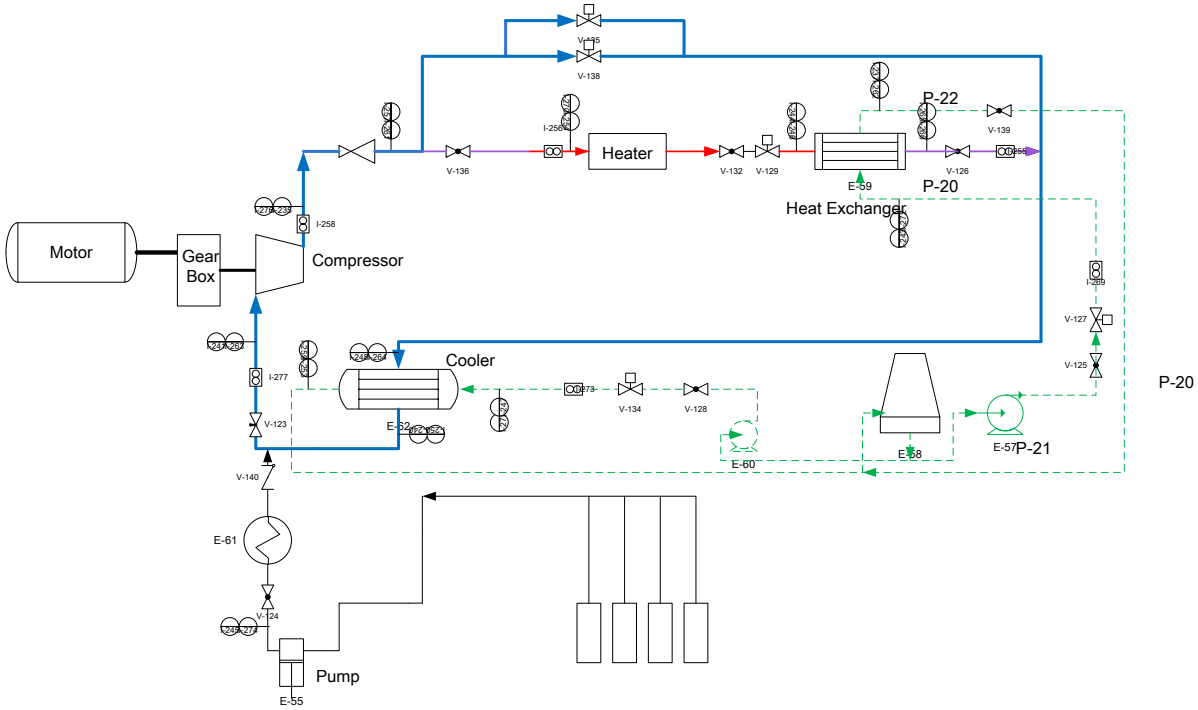

Fig1. The schematic of compressor test loop

TABLE 1. Design Point Specification for the sCO2 Compressor

Item	Value
Inlet Total Pressure	7.4Mpa
Inlet Total Temp.	32℃
Mass flow rate	55kg/s
Pressure ratio	1.9

2. COMPRESSOR AERODYNAMIC DESIGN

According to the design point parameters, a preliminary compressor rig flow-path is designed by the AxCent software and CFD analysis is performed by NUMECA software. Fig 2 shows the computation grid and Fig 3 shows the characteristics of the compressor, which indicates that the calculation result matches well with the design point. The static temperature, static pressure and density contours of the meridian plane are shown in Fig 4. It should be noted that in some tip region sCO2 will under the “dome” due to the acceleration.

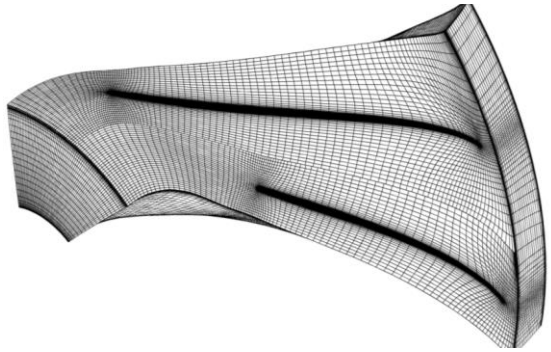

a. impeller

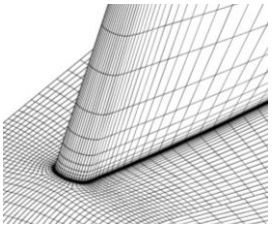

b. leading edge

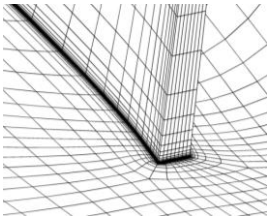

c. trailing edge

Fig 2 Computation grid

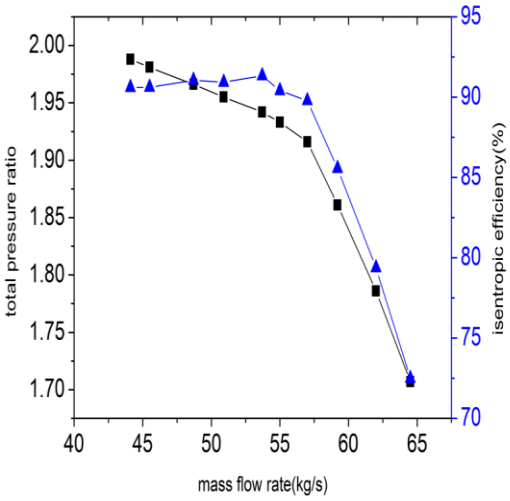

Fig 3 Characteristic of the compressor

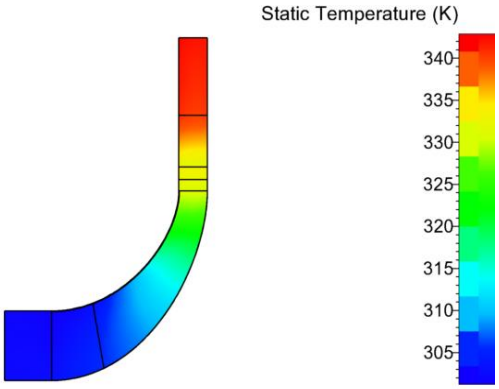

a. static temperature contour

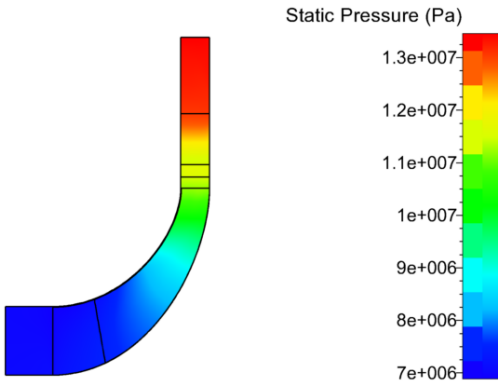

b. static pressure contour

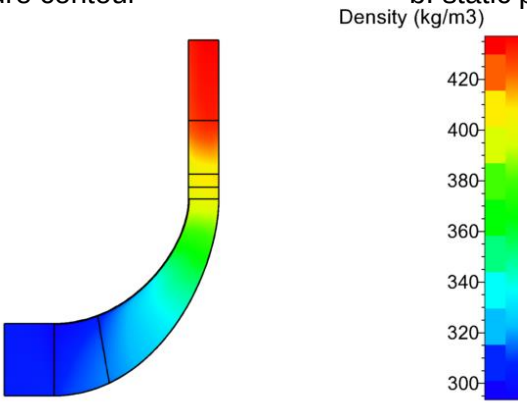

c. density contour

Fig 4 Meridian plane flow field

3. THE STRUCTURE DESIGN OF THE ROTOR

For the current sCO2 compressor test rig, the impeller, diffuser and the volute are designed with easy-to replace structure. The principal features of the compressor include the compressor rotor, shown in Figure 5, and consists of a single stage radial compressor impeller, dry gas-type shaft seal, hydro dynamic bearings, mechanical thrust bearing and coupling.

3.1 Rotor Dynamics Analysis

The rotor shown in Figure 5 has a calculated mass of 18.07 kg. The rotor dynamics proceeded according to ISO 1940 G2.5 standards and thus a calculated total residual imbalance allowance of 0.0172 kg-mm determined for a speed of 25,000 rpm. The two variants of this rotor were reviewed with the imbalance imposed at the impeller as shown in Figure 6.

Results of the rotor dynamics indicated that the variants 6A and 6B have very similar whirl speed and stability maps at nominal bearing diametral clearance 0.097 mm. Both variants are stable with positive log decrement in all range of rotational speed. Both variants 6A and 6B were shown to be stable with decreased bearing stiffness and damping coefficient while diametral clearance were also increased from 0.098 mm to 0.0121 mm. Log decrement was positive (above 2) in all range of rotational speed. The rotor dynamics was repeated with a heavier coupling (6.1 kg vs. 4.0 kg) and found to not increase rotor response. The effect of aerodynamic cross coupling was found to not affect rotor stability. Given these results of the rotor dynamics on the several design iterations, the rotor design is acceptable.

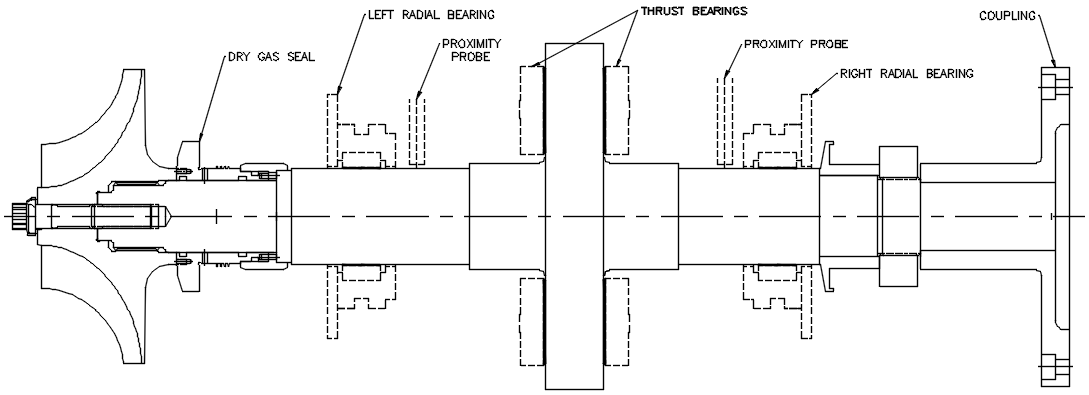

Figure 5. Major elements of the compressor rotor

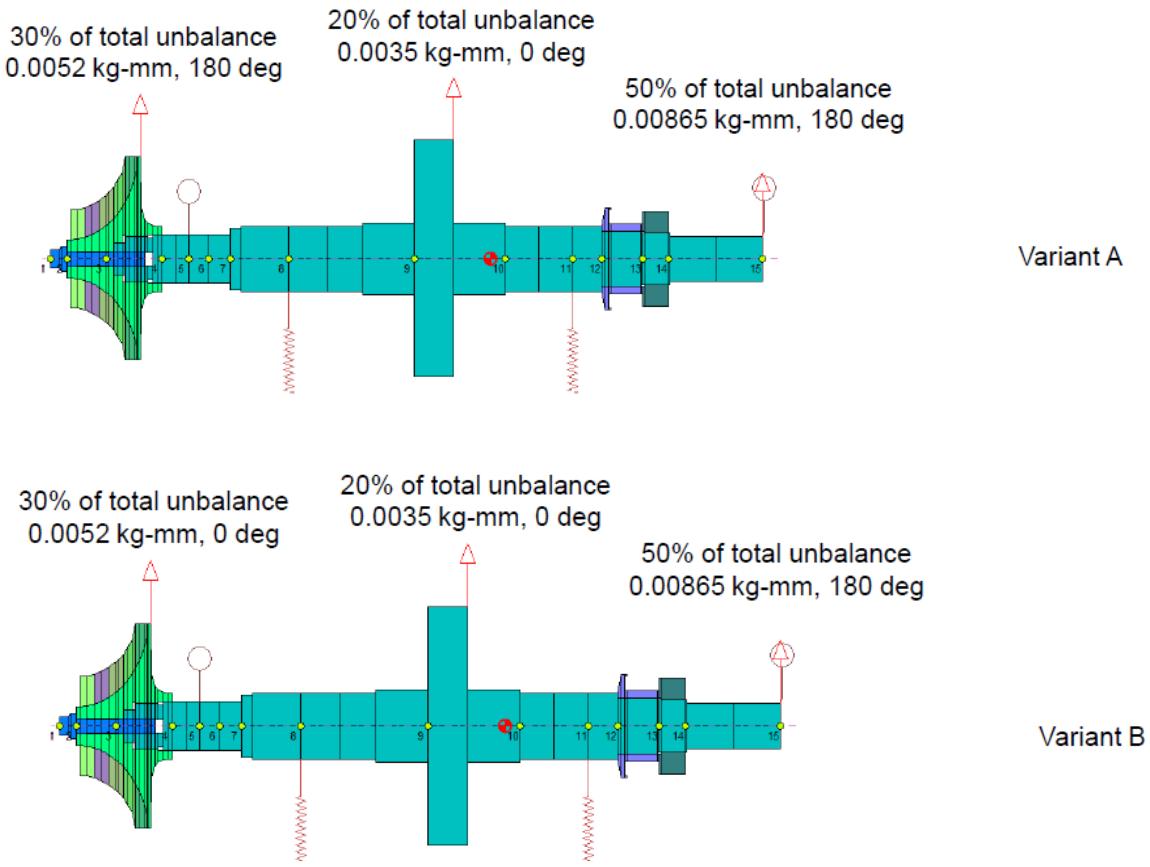

Figure 6. Details of Variants A and B that were considered during the rotor dynamics analysis

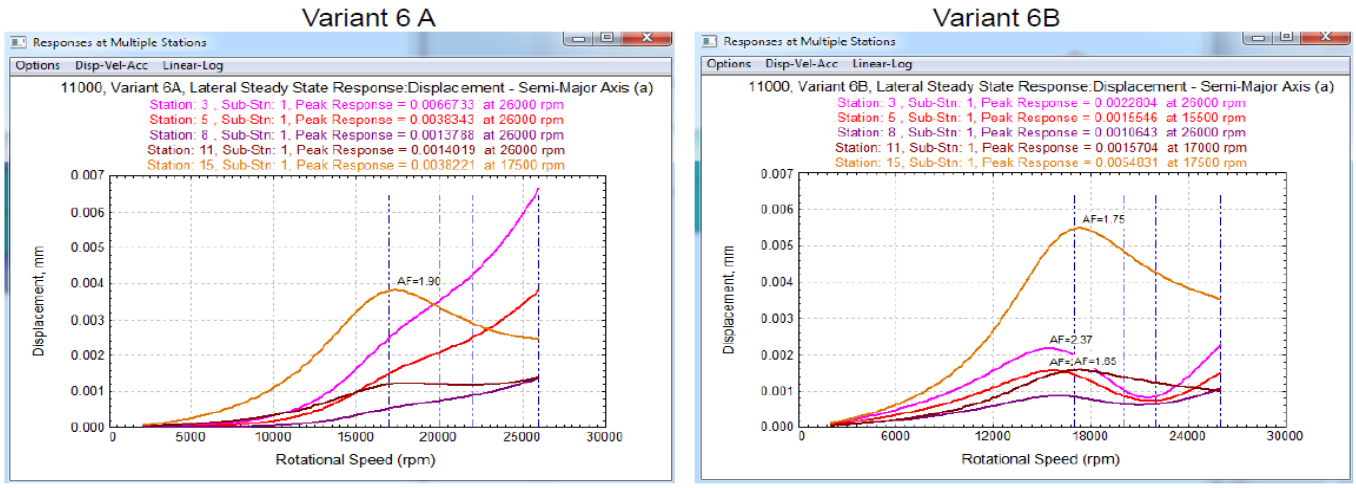

Station 1.....Impeller
Station 5.....gas seal
Station 8.....left bearing
Station 11.....right bearing
Station 15.....coupling

Figure 7. Steady State Response Displacement at Multiple Stations

3.2 Compressor Impeller Structural Design and Modal Analysis

A preliminary set of finite element analyses was performed to analyze the structural performance of the compressor impeller flow path configuration with 7 main and 7 splitter blades at a continuous 10% overspeed condition of 22,000 rpm using ANSYS® Mechanical v18.2.

For the Steady-State Thermal Analysis the surface temperature distribution along the flow path was mapped from the CFD analysis. For the Linear Static Structural Analysis, a 10% overspeed rotational velocity of ω = 22,000 rpm is applied as centrifugal loading. The rotor sector shown in Figure 8 used a body temperature distribution imported from a steady-state thermal analysis. The surface pressure distribution along the flow path was mapped from CFD analysis provided by SARI. The Prestressed Modal Analysis included a cyclic symmetry modal analysis using stress input from linear static structural analysis.

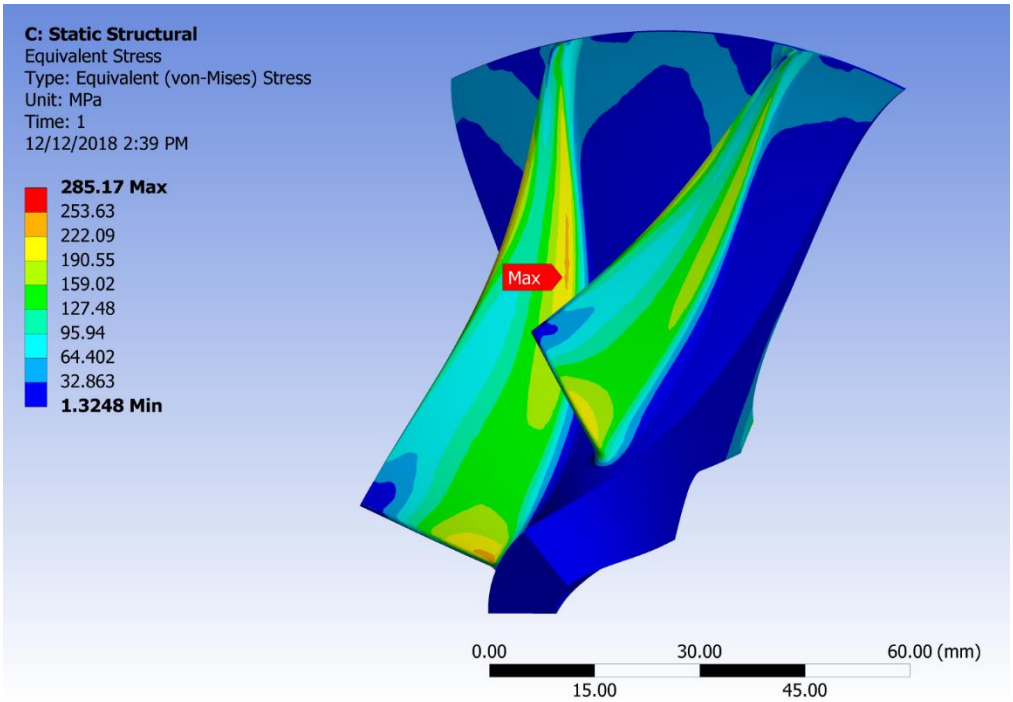

Figure 8. Impeller Sector used in the structural analysis of the sCO2 compressor

The results of the structural analysis shown in Table II indicated that the peak von Mises stress occurs at the main blade hub fillet region on the pressure side, with the peak von Mises stress being 77% of the local material yield strength at the 22,000 rpm 10% overspeed was significantly below the local yield strength for Aluminum 7075-T6 impeller material. Al-7075 T6 was also selected as the candidate impeller material due to its good corrosion resistance as well as its successful precedence as the material of choice for compressors used with sCO2 at temperatures below 100C allowing significant stress for the 22,000 rpm overspeed condition.

The structural analysis also indicated that the radial and axial deflections at the tips are well below the running clearance of 0.20 mm.

TABLE II. Results of the structural FEA for the compressor impeller sector shown in Figure 3

Quantity	Value
s_{von} (max)	285 MPa
s_Y (~50°C)	370 MPa
Max von Mises stress as % of Yield Strength	**77%**

A Modal (frequency response) Analysis was completed on the compressor impeller as shown in Figure 9. The analysis indicated that there is one potential interference mode, i.e., a main blade, primary blade-flapping mode at 4,585 Hz is within +6% of the 13x diffuser vane passing excitation frequency (4,333 Hz). The +6% is less than the normal allowance range of +/- 10% and thus warrants some attention. For example, modifying the blade thickness distribution at the hub will elevate the primary blade-flapping mode frequency above ±10% error margin. With the implementation of this viable modification of the blade geometry, the impeller design was considered acceptable.

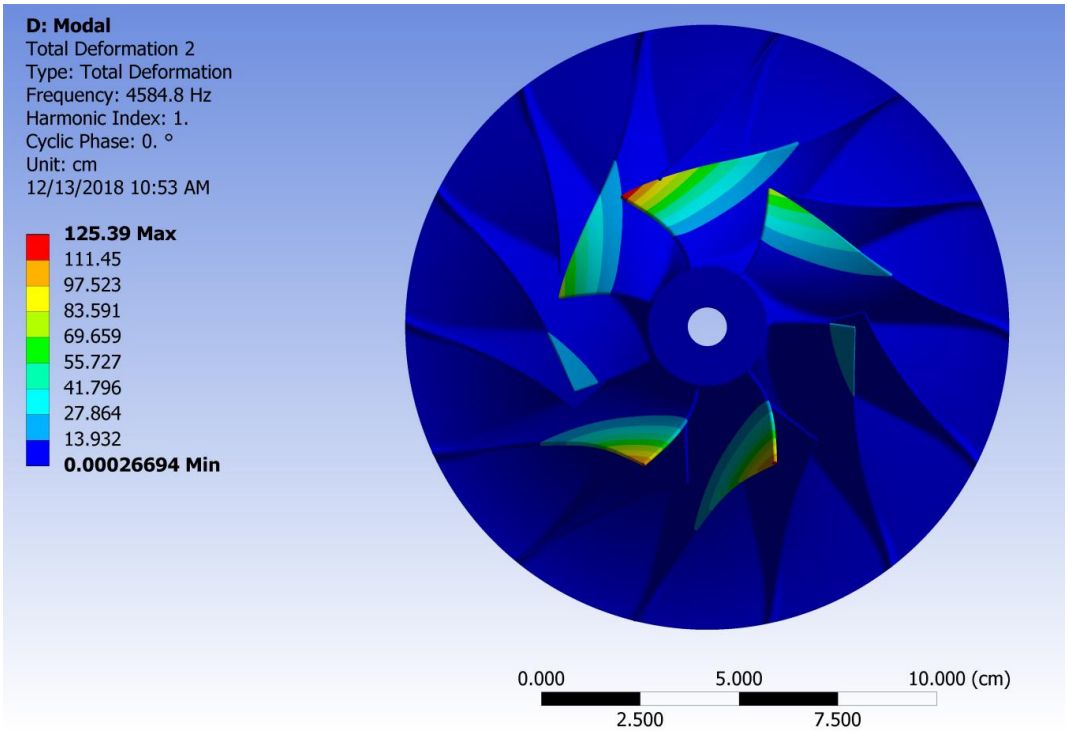

Figure 9. Display of Modal Analysis on compressor impeller indicating a possible blade flapping concern at 4,585 HZ (equal to 13 x diffuser vane passing frequency)

3.3 Compressor Casing Conceptual Design

The compressor casing design allowed for the necessary internal volute and included an FEA that demonstrated adequate safety margins. The FEA proceeded with a successful mesh density as shown in Figure 10. The finite element model was created in ANSYS® Mechanical™ v19.2 for the FEA. The bolts were modeled using beam elements within ANSYS with a prescribed pretension of 178 kN. Boundary conditions assigned include internal pressure, as well as forces associated to piping connected to various flanges. The finite element model shown in Figure 10 was generated using 150,000 quadratic tetrahedral elements. A proof pressure of 23.4 MPa was chosen based on a casing rating of 18 MPa x 1.3 ASME test multiplier.

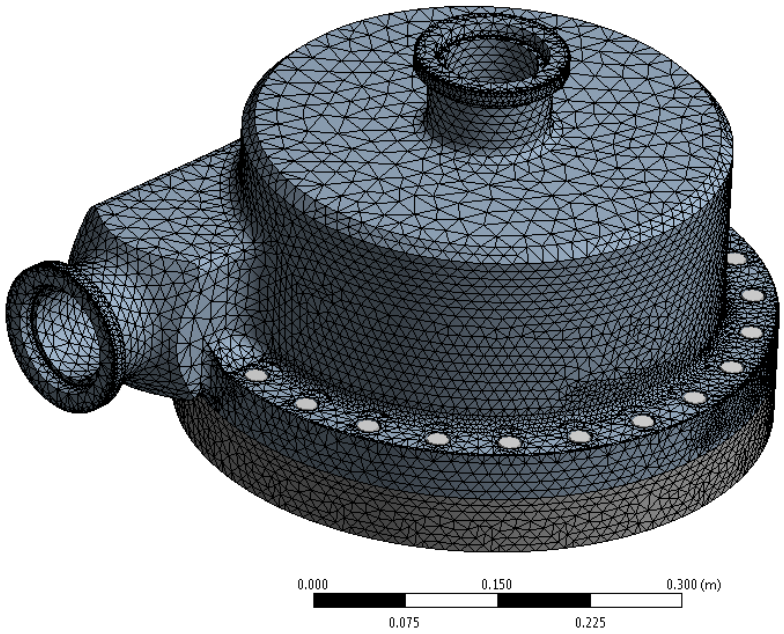

Figure 10. Illustration of Compressor Casing Design and successful FEA mesh density

The principal result of the FEA is displayed in Figure 11. The stresses in the casing are well below a singular "hot spot' of 450 MPa located in the small fillet around the bolt circle. Bulk stresses are well below 250 MPa. The peak von Mises stress of ~680 MPa occurs in the interface between the bolt and the casing, not shown in Figure 11. However, this stress concentration is artificial due to the simplification used in the modeling of the bolt in the current finite element model.

The Predicted stress versus yield stress or Margin of Safety is 1.85 Margin of Safety at Casing Rating {540 MPa /380 MP- from Figure 10 shown as light green) x 1.3}. This corresponds to a 2.4 M.O.S. (1.85 x 18 MPa/14.06 MPa) with respect to a 14.06 MPa Operating Pres.

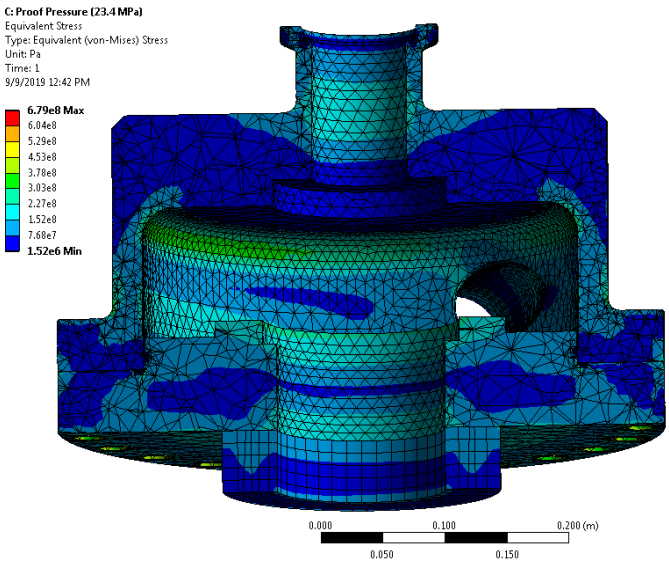

Figure 11. FEA result presenting the acceptable von Mise stress in the compressor casing

4. DESCRIPTION OF THE INSTRUMENTATION PLAN

The instrumentation plan includes those measurements essential for the determination of compressor stage performance. It also includes a minimum set of measurements for the possible determination of stage internal conditions needed to judge the separate performance of the key internal sections of the compressor.

In order to determine compressor performance, one must measure rotational speed, mass flow rate, inlet and exit pressures and inlet and exit temperatures. One may determine work input via the measurement of drive torque that is solely caused by the fluid process. Table III gives the corresponding measure device.

Table III. The Instrumentation Set

Parameter	Instrumentation Type
Mass flow rate	Coriolis Mass flowmeter
Torque	Torque Flange
Total Pressure	Kiel Probes
Static Pressure	Wall Static Pressure Taps
Temperature	Thermocouple
Unsteady Pressure	Kulite Transducer

5. CONCLUSION AND FUTURE WORK

The first Phase of this project is complete, and SARI is proceeding to the fabrication of the Compressor and integrate it into the Test Lab as shown in Figure 1. Work is proceeding to prepare detailed manufacturing drawings of the compressor rig. The procurement of materials for the compressor and the test facility is expected to be completed by March 2020. The compressor and instrumentation will be assembled before June, 2020. Testing will proceed immediately and continue to gather performance data to determine the actual static to static and static to total efficiencies of the compressor and the mechanical operation of the shaft seal. Tests will also

be conducted to validate several sCO2 Start-Up and Shut-Down sequence scenarios to determine the effect on the compressor surge and the need for fluid inventory control.

6. ACKNOWLEDGEMENTS

This study is financially supported by Key Laboratory of Low Carbon Conversion Science and Engineering, Chinese Academy of Sciences, Grant No. 119900DTZ3.

7. REFERENCES

[1] Jiang Mianheng, Xu Hongjie, *Advanced Fission Energy Program-TMSR Nuclear Energy System*. China Academic Journal, Vol，27(3), 2012: 366-374.

[2] Zhang Jingxuan, Ke Tingfeng, Zhu Yubo, Huang Weiguang, *A Design of Helium Closed Brayton Cycle Test Loop*. ACGT2014-129